

# Energy and Exergy Analysis of a Combined Power Generation System Using PEM Fuel Cell and Kalina Cycle System 11

Vahid Rezaee<sup>1</sup>, Arash Houshmand<sup>2\*</sup>

Received 01 June 2015; accepted after revision 04 August 2015

## Abstract

*This paper presents an energy and exergy analysis of a combined power generation system consists of a Proton Exchange Membrane fuel cell (PEMFC) power station and Kalina cycle system 11 (KCS11) that converts low temperature waste heats into electricity. The application of this combined system is high efficiency electric power generation in a power station. The energy and exergy analysis of the Hybrid power system is carried out to determine the possible improvement of system. Results show that the energy and exergy efficiencies of the combined system, as compared to the PEM fuel cells stack power station without KCS11, are improved about 1.75% and 1.5%, respectively.*

## Keywords

*Energy and exergy analysis, hybrid power systems, KCS11, PEM fuel cell stack*

## 1 Introduction

The fuel cells are green technologies that generate electricity through electrochemical processes. Fuel cell stacks operate silently, produce no pollutants (produce only heat and water as waste products), have simple maintenance due to few moving parts in the system, provide high quality DC power and have high degree of reliability [1]. On the other hand, the fuel cells have some disadvantages, such as difficult fuelling, system complexities and expensive to produce. The advantages of fuel cells can overcome the disadvantages and they could become the first choice for many future applications with lower cost[2]. The possible applications of PEM fuel cells are generating required power for automobiles, submarines, power stations, air conditioners and combined heat and power (CHP) applications [3, 4]. Among all types the fuel cells, the highest power density and specific power can be find in PEM fuel cells specifications [5]. The stationary application of PEM fuel cells has a wide range of 1-50 MW [2].

Generally, a cathode and an anode beside an electrolyte are the main part of a fuel cell. During an electrochemical reaction the chemical energy is converted to electrical energy [6]. In this study the aim of PEM fuel cells application is to generate the electric power in a power station for a city. The bipolar plates are used in the stack when several cells are connected in series. In order to the hydrogen and oxygen gases flow over the face of the anode and cathode electrodes, special channels are made in the bipolar plates [7].

Nowadays, there is a tendency towards utilizing the waste heat of PEM fuel cells as electricity which is transportable, storable and clean [8,9]. The kalina Cycle System 11(KCS11) that was introduced by Dr. Alexander Kalina [10] is a good idea for converting low temperature waste heats into electricity. The KCS11 utilizes a water-ammonia mixture as the working fluid. A schematic of the KCS11 is presented in Fig.1. At state 5, the mixture (saturated vapour) leaves the evaporator. Then the mixture passes through the separator. At this moment the separator separates the working fluid into two separate streams. The saturated vapour produces work on the turbine. At state 7 the liquid part of the working fluid leaves the separator and enters

<sup>1</sup>Department of Mechanical Engineering, Mohaghegh Ardabili University, Ardabil, Iran

<sup>2</sup>Department of Mechanical Engineering, Science and Research Branch, Islamic Azad University, Tehran (Markazi), Iran

\*Corresponding author, e-mail: [arash.houshmand@live.com](mailto:arash.houshmand@live.com)

the regenerator. The liquid in regenerator is cooled by mixing with the cooled liquid that has left the condenser. At state 8, through an expansion valve, the liquid pressure is dropped. The outlet liquids at state 9 and state 10 enter the absorber. At state 1 the mixture leaves the absorber and enters the condenser. At the condenser, the heat of mixture is rejected and at state 2 it leaves the condenser. The compressed mixture is pumped to the regenerator at state 3. The mixture leaves the regenerator at state 4 and it reaches to the evaporator in order to repeat the process. [11]

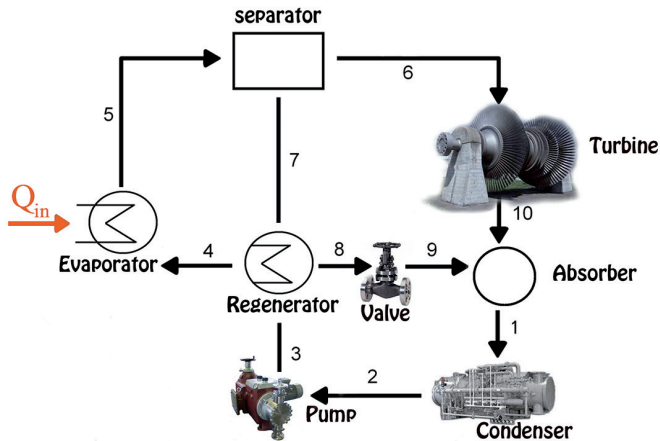


Fig. 1 Schematic diagram of the KCS11

The main focus of KCS11 researches is on the modification and optimization of cycle and NH<sub>3</sub>-H<sub>2</sub>O mixture [12-14].

One of the best ways to evaluate the performance of energy systems is the study on energy and exergy efficiencies [15]. The presented study deals with the analysis of an energy system, consisting of 13000 PEM fuel cells combined with KCS11 to use the waste heat of the fuel cells in a power station.

## 2 Hybrid Power System Description

In Figure 2 the schematic of the combined power system is shown using PEMFC and KCS11.

The system operation shown in Fig. 2 can be summarize as [16,17]:

The air pressure is increased up to a desired operating pressure by compressor then is supplied to the cathode and in other side the pressure of hydrogen is reduced by pressure regulator then it is fed to the anode. At state 5 the heated ammonia–water solution is passed through the separator and the separator separates the saturated vapour from the liquid. The vapour is fed to the turbine at state 6 and the liquid is fed to the regenerator at state 7. At state 8 through an expansion valve the liquid pressure is dropped and it is fed to the absorber at state 9. The turbine products electricity and the weaker mixture (ammonia–water) is fed to the absorber at state 10. At State 1 the mixture (ammonia–water) is condensed through the condenser and at state 2 it enters the pump. At state 3 the mixture (ammonia–water) is pumped to the regenerator. The mixture returns to the cycle at state 4 in order to capture the waste heat of the cells and start the process over again.

## 3 Modelling of Hybrid Power System

To create a model for the hybrid system it is assumed that the system reaches the steady state, the pressure drops are negligible, environmental heat transfer is waived, the fuel cell operating temperature is 85°C, the chemical composition of Air consists of 79% N<sub>2</sub> and 21% O<sub>2</sub>, [17,18].

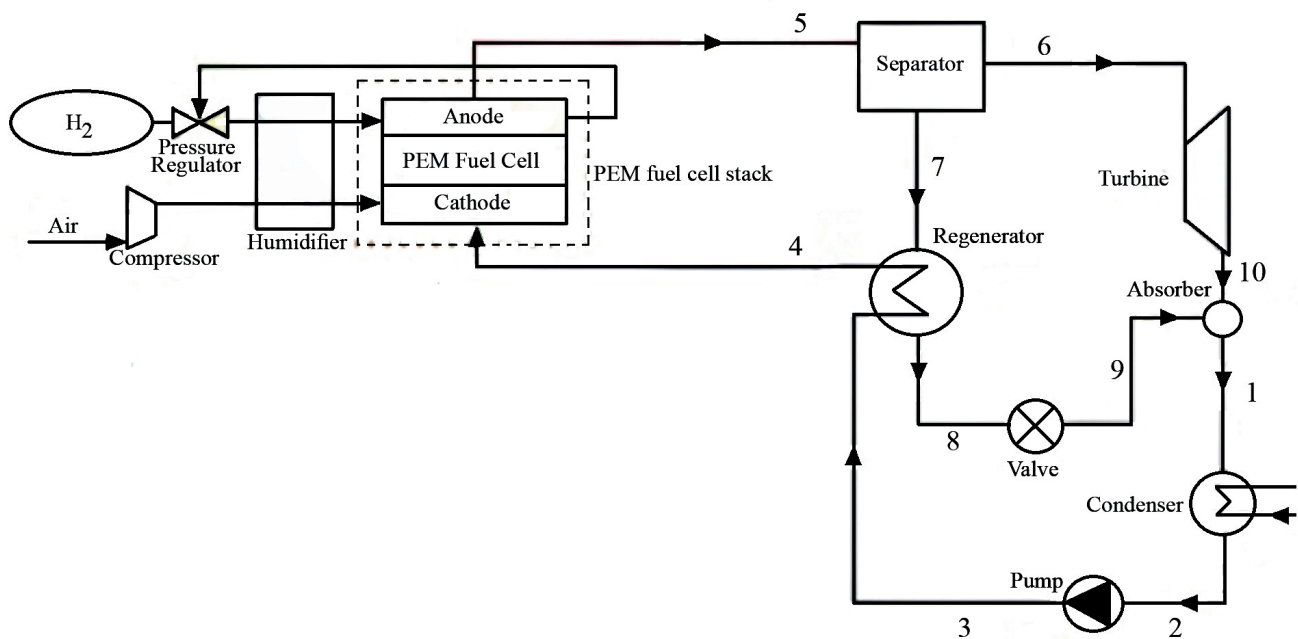


Fig. 2 Schematic of combined power system.

### 3.1 PEMFC Mathematical Model

Generally overall reaction inside the PEMFC is defined as:



The system is reversible thus the electromotive force or reversible open circuit voltage of the FC is defined as:

$$E = -\frac{\Delta G_f}{2F} \quad (2)$$

Where, E: the open circuit voltage of cell (V),  $\Delta G_f$ : the change of Gibbs free energy (Jol/mol), F: the Faraday constant (96,485 °C/mol).

The actual output voltage of the PEMFC is the sum of Nernst voltage, activation overvoltage, Ohmic losses and concentration overvoltage and calculated as:

$$V_{FC} = E_N + V_a + V_o + V_c \quad (3)$$

Where,  $V_{FC}$ : the actual output voltage of the FC (V),  $E_N$ : the Nernst voltage (V),  $V_a$ : the activation overvoltage (V),  $V_o$ : the ohmic losses (V),  $V_c$ : the concentration overvoltage (V).

The PEMFC Nernst voltage is the reversible cell voltage at a given temperature and pressure and calculated as [19]:

$$E_N = E^\circ - 0.85 \times 10^{-3} (T_{cell} - 298.15) + 4.31 \times 10^{-5} T_{cell} \left[ \ln(p_{\text{H}_2}^{\text{contact}}) + 0.5 \ln(p_{\text{O}_2}^{\text{contact}}) \right] \quad (4)$$

Where,  $E^\circ$ : The electromotive force at standard pressure and pressure (=1.229V),  $T_{cell}$ : The cell temperature (K),  $p_{\text{H}_2}^{\text{contact}}$ : the hydrogen partial pressure (bar),  $(p_{\text{O}_2}^{\text{contact}})$ : the oxygen partial pressure (bar).

Activation overvoltage is the cause of voltage drop and irreversibility and at lower temperatures and pressures it becomes more important. It is calculated as [20]:

$$V_a = \delta_1 + \delta_2 T_{cell} + \delta_3 T_{cell} \ln \left( 1.97 \times 10^{-7} P_{\text{O}_2} \exp \left( \frac{498}{T_{cell}} \right) \right) + \delta_4 T_{cell} \ln(I) \quad (5)$$

Where,

$$\delta_1 = -0.948$$

$$\delta_2 = 0.00286 + 0.0002 \ln(A_{cell})$$

$$+ 4.3 \times 10^{-5} \ln 9.174 \times 10^{-7} P_{\text{H}_2} \exp \left( \frac{-77}{T_{cell}} \right)$$

$$\delta_3 = 7.6 \times 10^{-5}$$

$$\delta_4 = -1.93 \times 10^{-4}$$

The ohmic loss occurs due to the electrical resistance caused by the electrolyte. According to ohm's law the Ohmic losses is defined as:

$$V_o = IR \quad (6)$$

The mass transport or concentration overvoltage is occurs due to change in the concentration of the reactants at the surface of the electrodes and it is calculated as:

$$V_c = m \exp(ni) \quad (7)$$

Where,  $m = 3 \times 10^{-5}$ (V),  $n = 8 \times 10^{-3}$  (cm<sup>2</sup>/mA), i: the stack operating current density (A/cm<sup>2</sup>)

PEMFC stack output power from the well-known formula (Power = VI) is calculated as:

$$W_{fc} = N_{cell} V_{fc} I \quad (8)$$

### 3.2 PEM Fuel Cell Thermal Model

Mass balance of the PEMFC is defined as:

$$\sum (m_i)_{in} = \sum (m_i)_{out} \quad (9)$$

The rate of gas usage in the cell is related to the current. Consumption rate of hydrogen, oxygen and air respectively are defined as:

$$\dot{n}_{\text{H}_2, \text{con}} = \frac{I}{2F} \quad (10)$$

$$\dot{n}_{\text{O}_2, \text{con}} = \frac{I}{4F} \quad (11)$$

$$\dot{n}_{\text{H}_2\text{O}, \text{gene}} = \frac{I}{2F} \quad (12)$$

Where, I: the operating Current (A), F: the Faraday constant (96,485 °C/mol)

Mass flows of inlet air and inlet hydrogen are defined as:

$$\dot{m}_{\text{air}, in} = 3.57 \times 10^{-7} \left( \frac{\lambda_{\text{air}} W_{fc}}{V_{FC}} \right) \quad (13)$$

$$\dot{m}_{\text{H}_2, in} = 1.05 \times 10^{-8} \left( \frac{W_{fc}}{V_{FC}} \right) \quad (14)$$

Where,  $\lambda_{\text{air}}$ : the stoichiometry Rate of the air (-).

The net heat energy must be removed from the cell in order to avoid overheating. thermodynamic balance equation of net heat energy of PEM Fuel cell as [18]:

$$\dot{Q}_{net} = \dot{Q}_{chem} - W_{fc} - \dot{Q}_{sens+latent} \quad (15)$$

The net heat energy is transferred to the KCS11 in order to recover the waste heat.

Under the steady state, the input exergy will be equal to the sum of the output exergy, exergy destruction and exergy loss so the exergy balance equation is defined as:

$$\dot{E}_{x,in} = \dot{E}_{x,out} + \dot{E}_{x,D} + \dot{E}_{x,loss} \quad (16)$$

The input and output exergy rates are respectively calculated as Equations (17) and (18) [21]:

$$\dot{E}_{x,in} = \sum_i \dot{m}_{i,in} e_x + \dot{W}_{in} + \sum_i \dot{Q}_{i,in} \left(1 - \frac{T_0}{T_i}\right) \quad (17)$$

$$\dot{E}_{x,out} = \sum_i \dot{m}_{i,out} e_x + \dot{W}_{out} + \sum_i \dot{Q}_{i,out} \left(1 - \frac{T_0}{T_i}\right) \quad (18)$$

Where,  $e_x$ : the total Specific Exergy (J/kg) which is the total exergy of a stream on a unit of mole.

The difference between the enthalpy and entropy from the standard conditions can be found in the physical exergy. The physical exergy when the velocity and elevation are neglected [22] is defined as:

$$e_{x,ph} = (h - h_0) - T_0(s - s_0) \quad (19)$$

Where,  $h$ : enthalpy (kJ/kg),  $h_0$ : specific enthalpy (kJ/kg),  $s$ : entropy (J/kg K),  $s_0$ : specific entropy (J/kg K)

The departure of the chemical composition of the PEMFC in working condition from that of the environment, deals with the chemical exergy. The Chemical exergy of the PEMFC is calculated as:

$$e_{x,Ch} = \sum x_n e_{x,n}^{ch} + RT_0 \sum x_n \ln x_n \quad (20)$$

The transferred net heat energy of the PEMFC stack to KCS11 from Fig. 2 is calculated as:

$$\dot{Q}_{fc} = \dot{Q}_{net} = \dot{m}(h_5 - h_4) \quad (21)$$

The electrical efficiency of the PEMFC is defined as the ratio of the net power output to the electrochemical reaction power [18,23], so it can be defined as:

$$\eta_{FC} = \frac{W_{fc} - W_{com}}{\dot{n}_{H2,consumed} HHV} \quad (22)$$

Where, HHV: the higher heating value of hydrogen (kJ/mol).

The total exergy transfer is expressed as the sum of the specific physical, chemical, kinetic and potential exergies which the potential and kinetic exergies can be neglected [23]. Therefore the PEMFC stack electrical exergy efficiency is defined as the ratio of the net power output to the sum of the specific physical and chemical exergies, so it can be expressed as:

$$\eta_{ex,FC} = \frac{W_{fc} - W_{com}}{\left[ \dot{m}(e_{x,ph} + e_{x,Ch}) \right]_{H2,in}} \quad (24)$$

### 3.3 Energy and Exergy analysis of KCS11

From Figure 2, Energy balance in separator and absorber are calculated as seen in Equations (24) and (25), respectively:

$$(h_5 - h_6) = x_{sep}(h_7 - h_6) \quad (25)$$

$$(h_1 - h_{10}) = x_{abs}(h_9 - h_{10}) \quad (26)$$

Where,  $h$ : enthalpy (kJ/kg),  $x$ : mass fraction through specified state(-).

From Figure 2, Energy in turbine and pump respectively are calculated as in equations (26) and (27):

$$\dot{W}_{turb} = \dot{m}(h_6 - h_{10}) \quad (27)$$

$$\dot{W}_{pump} = \dot{m}(h_3 - h_2) \quad (28)$$

From Figure 2, exergy in turbine and pump respectively are calculated as equations (28) and (29):

$$\dot{E}_{dest,turb} = \dot{m}(e_{x,ph,6} - e_{x,ph,10}) - \dot{W}_{turb} \quad (29)$$

$$\dot{E}_{dest,pump} = \dot{W}_{pump} - \dot{m}(e_{x,ph,3} - e_{x,ph,2}) \quad (30)$$

### 3.4 Energy and Exergy analysis of combined system

The electrical efficiency of the combined system is defined as the ratio of the net power output of the combined system to the electrochemical reaction power, can be expressed as:

$$\eta_{elec} = \frac{W_{fc} + W_{turb} - W_{pump} - W_{com}}{\dot{n}_{H2,cons} HHV} \quad (31)$$

The Electrical exergy efficiency of the combined system is defined as the ratio of the net power output to the sum of the specific physical and chemical exergies, so it can be expressed as:

$$\eta_{ex,elec} = \frac{W_{fc} + W_{turb} - W_{pump} - W_{com}}{\left[ \dot{m}(e_{x,ph} + e_{x,Ch}) \right]_{H2,in}} \quad (32)$$

## 4 Validation of the Model

In order to confirm the model, the results obtained by other references are presented to ensure the accuracy of the model. The results of model demonstrate good consistency with [18], [23], and [24] models.

The key assumptions and parameters for hybrid power system model are listed in table1. The modelling results along with the values reported by references are indicated for individual fuel cell stacks in Table 2, individual KCS11 in Table 3, and hybrid system power based on fuel cell and KCS11 are presented in Table 4.

**Table 1** Combined power generation system parameters specifications [18].

Parameter	Value	Parameter	Value
Electrons Number (-)	2	Universal gas constant (J/mol K)	8.314
Faraday constant (°C/mol)	96458	Ambient temperature (K)	298
Stack temperature (K)	358	Membrane thickness (cm)	0.00254
PEM fuel cell pressure (bar)	3	Hydrogen Stoichiometry Rate (-)	1.2
Number of stack cells	13000	Current transferring density(A/cm <sup>2</sup> )	10 <sup>-6.912</sup>
Active surface area (cm <sup>2</sup> )	232	Air specific heat capacity(J/ kg K)	1005
Air Stoichiometry Rate (-)	2	Hydrogen Specific heat capacity (J/kg K)	14300
Stoichiometric rate of hydrogen (-)	1.2	Ideal efficiency of Turbine (%)	85
current density of PEM fuel cell stack (A cm <sup>-2</sup> )	0.6	Ideal efficiency of Pump (%)	70

**Table 2** Mathematical modeling. Results.

Parameter	Results	Results reported by A. Yilanci et al. [23]	Results reported by P. Zhao et al. [18]
Open circuit voltage of the system (V)	1.229	1.229	1.229
Nernst voltage (V)	1.177	1.173	-
Activation overvoltage (V)	-0.4378	-	-
Ohmic overvoltage (V)	0.002289	-	-
Concentration overvoltage (V)	0.003645	-	-
Cell operating voltage (V)	0.6857	-	0.653
Stack electrical net output power (KW)	1241	1200	1006.7
Compressor power (KW)	157.4	-	175.59
PEM fuel cell stack energy efficiency (%)	40.45	42.17	37.59
PEM fuel cell stack exergy efficiency (%)	35.51	38.12	-

**Table 3** The results of individual KCS11 analysis

Parameter	Results	Results reported by H. M. Hettiarachchi et al. [24]
Turbine output power (kW)	49.75	-
Pump power (kW)	2.887	-
Energy efficiency (%)	10.21	10.21
Exergy efficiency (%)	26.71	-

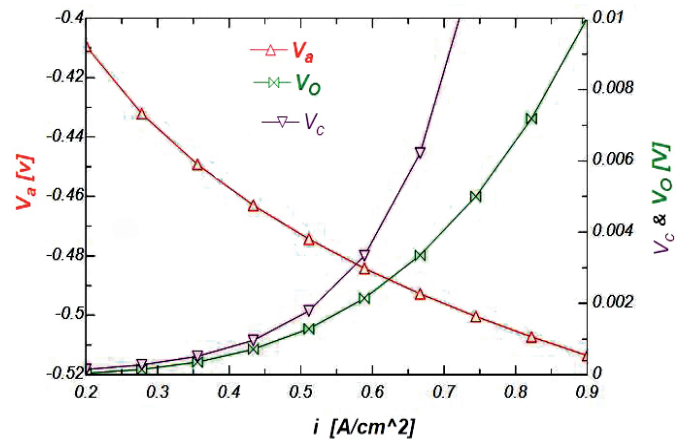
**Table 4** The results of hybrid power system analysis

Parameter	Results
Net power (kW)	1130
Electrical energy efficiency (%)	42.2
Electrical exergy efficiency (%)	37.05
Hybrid power system improvement efficiency (%)	1.75

## 5 Results

Electrochemistry thermodynamics, as well as other thermodynamic relations are used to create a model for the combined power generation system based on PEMFC and KCS11; in the following section the results will be presented by related diagram and tables.

The variations of Activation, concentration and ohmic overvoltages at different current densities are shown in Fig. 3. As Figure 3 illustrates, the concentration and ohmic polarization losses directly, and activation polarization is inversely proportional with current density. The activation polarization for each current density is higher than other losses, therefore, the activation polarization is considered as the largest voltage loss on PEMFC.

**Fig. 3** Activation, concentration and ohmic, losses.

The ohmic polarization diagram rises up when the density increases, though it is not significant. The concentration polarization exponentially rises with the current density. The numeric value of the voltage losses was shown in Table 4.

The current density vs. the actual output voltage of the PEMFC is shown in Fig. 4. The actual output voltage of the PEMFC varies between 0.6(V)-0.7(V) that is 0.6857(V) in this research obtained for the model. As Figure 4 shows, as current density rises, the output voltage of PEMFC will drop due to the polarization losses. The maximum output voltage of the PEMFC is placed at zero current density and in the continuance, it slopes down.

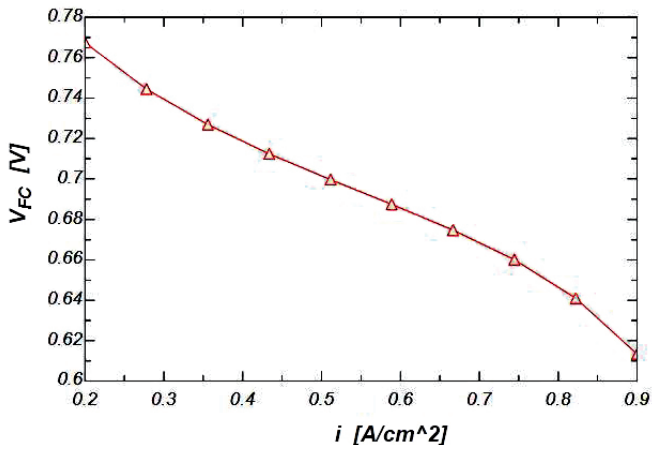


Fig. 4 The variations of the actual output voltages of the PEMFC at different current densities.

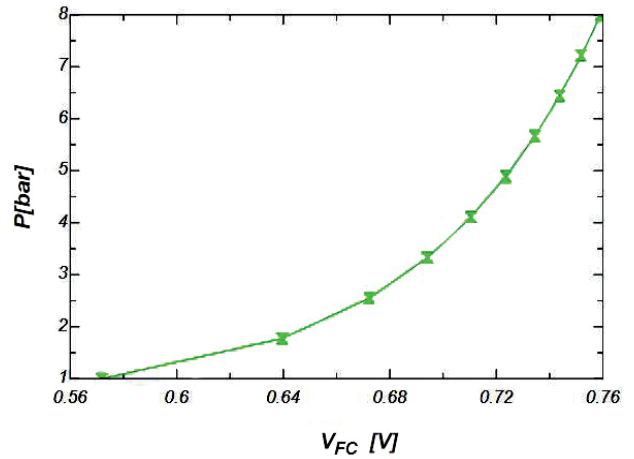


Fig. 6 The PEMFC pressure vs. actual output voltages of the PEMFC.

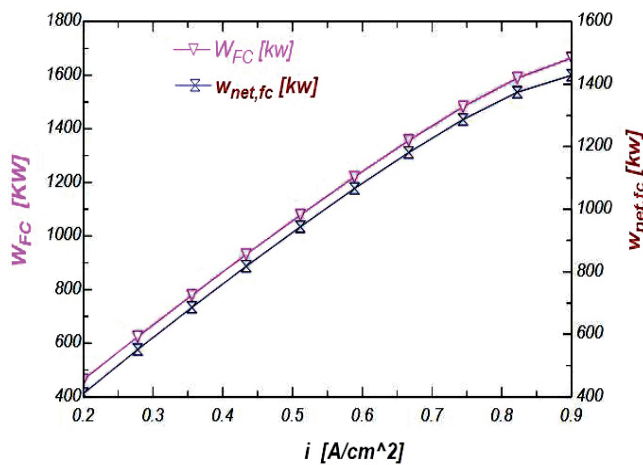


Fig. 5 The variations of output power by the PEMFC at different current densities.

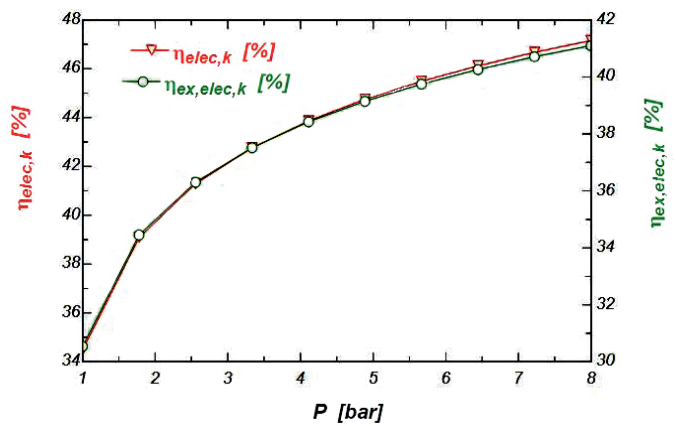


Fig. 7 The electrical energy and exergy efficiencies of the hybrid system vs. operation pressure of the PEMFC.

The direct proportional of the PEMFC output power and operating current density is shown in Fig. 5. In highest possible current density, output power will reach the maximum/peak value. In  $0.6(\text{A}/\text{cm}^2)$  current density, the PEMFC output power is obtained 1241 (KW).

The PEMFC pressure diagram vs. output voltages is shown in Fig. 6. The PEMFC operating pressure varies between 1bar up to 8 bars. The PEMFC actual output voltage is directly proportional to the PEMFC pressure.

The electrical energy and exergy efficiencies of the combined power system at different PEMFC operation pressure are shown in Fig. 7. The electrical efficiency of the combined power system is obtained 42.2%.

Fig. 8 and 9 show the final results of model analysis with energy diagram and the exergy destruction diagrams, respectively. From the point of energy, the highest loss exists in the fuel cell stack and the condenser of KCS11. However, from the point of exergy, the highest exergy destruction values are seen respectively on stacks, separator, and absorber. As results show in the presented cycle beside of energy generating there

are some energy losses that occur in any energy systems. The overall result of energy analysis shows that there is about 1.75% improvement after using KCS11 in combined power generation system.

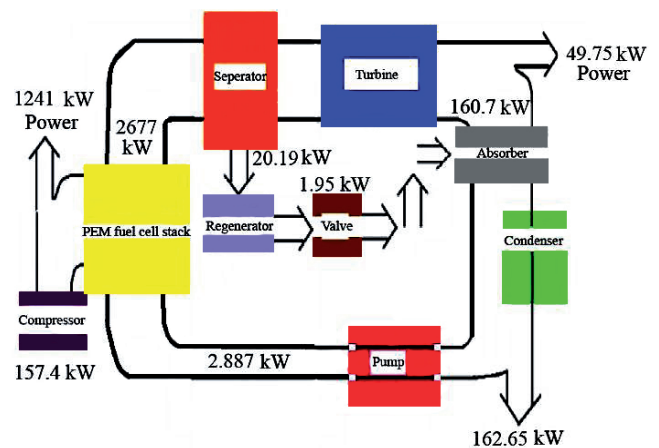


Fig. 8 The energy diagram of the combined power generation system model.

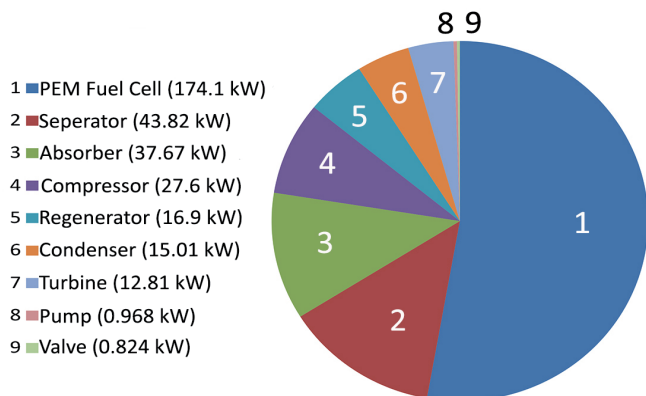


Fig. 9 the exergy destruction diagram of the combined power generation system model.

## 6 Conclusions

The application of PEMFC stack is a wide range of power generation of automobiles, air crafts and submarines to electric power generation in a power station of which the latter is under research view. KCS11 is used at large scales to generate electricity at power stations. A combined power generation system consists of PEMFC stack and KCS11 is presented in this study.

As a result of combination of these technologies, the energy and exergy efficiencies of combined power system show improvement as compared to the state when KCS11 is out of cycle. In energy analysis the electrical efficiency of the individual fuel cell, individual KCS11 and hybrid power system are obtained 40.45%, 10.21%, and 42.2%, respectively; therefore there is about 1.75% improvement for combined power generation system based on the PEMFC stack and the KCS11 compared to individual fuel cell and individual KCS11.

Moreover, the exergy analysis indicated that the exergy efficiency of the individual PEMFC stack and combined system are 35.51% and 37.05%, respectively; therefore exergy efficiency will be increased by about 1.5% in the hybrid system when both systems are mixed (the PEM stack and the KCS11). These results are theoretical probabilities which may be different from that of real practical conditions due to the assumptions on systems elements, efficiencies and other working conditions. So the use of this system is extremely depending on heeding the requirements of theoretical assumptions. In addition, the application of this combined cycle must have an economic justification due to the cost of the added cycle. So the profitability of system in energy generating must be overcome the cost of required equipment in the beneficial working period of the system.

## Acknowledgement

We would like to express our deep appreciation to Dr. Yaser Maddahi from the University of Calgary for his valuable comments during the preparation of present work.

## Notation

$C$	Specific Heat Capacity (J/mol K)
$E$	Voltage of Cell (V)
$\dot{E}_x$	Exergy (kW)
$e_x$	Total Specific Exergy (J/kg)
$F$	Faraday Constant ( $^{\circ}\text{C}/\text{mol}$ )
$HHV$	Higher Heating Value of Hydrogen (kJ/mol)
$h$	Enthalpy (kJ/kg)
$I$	Stack Operating Current (A)
$i$	Stack Operating Current Density ( $\text{A}/\text{cm}^2$ )
$\dot{m}$	Mass flow rate (kg/s)
$m_i$	Mass (kg)
$N_{cell}$	Number of cells
$n$	Numbers of Electrons
$\dot{n}$	Molar Flow Rate (mol/s)
$P$	Pressure (bar)
$Q$	Heat energy (J)
$R$	Cell Resistance ( $\Omega$ )
$s$	Entropy (J/kg K)
$T$	Temperature (K)
$V$	Voltage(V)
$W$	Output power (W)
$x$	Mass fraction (-)
$G$	Gibbs Free Energy (J/mol)

## Greek symbols

$\delta$	Activation Overvoltage coefficients (Empirical)
$\eta$	Efficiency (%)
$\lambda$	Stoichiometry Rate

## Subscripts

1,2,3,...,10	Points in Fig.2
$a$	Activation
$abs$	Absorber
$air$	Air
$c$	Condenser
$cell$	Cell
$ch$	Chemical
$comp$	Compressor
$com$	Compression
$conc$	Concentration
$cons$	Consumed
$FC$	Fuel cell
$gene$	Generation
$H_2$	Hydrogen
$H_2O$	Water
$in$	Input
$N_2$	Nitrogen
$O$	Ohmic
$out$	Output
$O_2$	Oxygen

<i>pump</i>	Pump
<i>ph</i>	Physical
<i>sep</i>	Separator
<i>turb</i>	Turbine

## Abbreviation

KCS11	Kalina Cycle System 11
PEM	Proton Exchange Membrane
CHP	Combined Heat and Power
FC	Fuel Cell

## References

- [1] Wang, C., Nehrir, M. H., Shaw, S. R. "Dynamic models and model validation for PEM fuel cells using electrical circuits." *IEEE Transactions on Energy Conversion*. 20(2), pp. 442-451. 2005. DOI: [10.1109/TEC.2004.842357](https://doi.org/10.1109/TEC.2004.842357)
- [2] Wang, Y., Chen, K. S., Mishler, J., Cho, S. C., Adroher, X. C. "A review of polymer electrolyte membrane fuel cells: technology, applications, and needs on fundamental research." *Applied Energy*. 88(4), pp. 981-1007. 2011. DOI: [10.1016/j.apenergy.2010.09.030](https://doi.org/10.1016/j.apenergy.2010.09.030)
- [3] Wee, J.-H. "Applications of proton exchange membrane fuel cell systems." *Renewable and sustainable energy reviews*. 11(8), pp. 1720-1738. 2007. DOI: [10.1016/j.rser.2006.01.005](https://doi.org/10.1016/j.rser.2006.01.005)
- [4] Yaldagard, M., Jahanshahi, M., Seghatoleslami, N. "Carbonaceous Nanostructured Support Materials for Low Temperature Fuel Cell Electrocatalysts-A Review." *World Journal of Nano Science and Engineering*. 03(04), 2013. DOI: [10.4236/wjnse.2013.34017](https://doi.org/10.4236/wjnse.2013.34017)
- [5] Patil, M. B., Bhagat, S. L., Sapkal, R. S., Sapkal, V. S. "A review on the fuel cells development." *Scientific Reviews & Chemical Communications*. 1, pp. 25-41. 2011.
- [6] Haile, S. M. "Fuel cell materials and components." *Acta Materialia*. 51(19), pp. 5981-6000. 2003. DOI: [10.1016/j.actamat.2003.08.004](https://doi.org/10.1016/j.actamat.2003.08.004)
- [7] Larminie, J., Dicks, A., McDonald, M. S. "Fuel cell systems explained 2." New York: Wiley. 2003.
- [8] Hendricks, T., Choate, W. T. "Engineering scoping study of thermoelectric generator systems for industrial waste heat recovery." *US Department of Energy*. 20. p. 6. 2006.
- [9] Ismail, B. I., Ahmed, W. H. "Thermoelectric power generation using waste-heat energy as an alternative green technology." *Recent Patents on Electrical Engineering*. 2(1), pp. 27-39. 2009. DOI: [10.2174/1874476110902010027](https://doi.org/10.2174/1874476110902010027)
- [10] Kalina, A. I. "Combined-cycle system with novel bottoming cycle." *Journal of engineering for gas turbines and power*. 106(4), pp. 737-742. 1984. DOI: [10.1115/1.3239632](https://doi.org/10.1115/1.3239632)
- [11] Jones, D. A. "A study of the Kalina cycle system 11 for the recovery of industrial waste heat with heat pump augmentation." Auburn University. 2011. URL: <http://hdl.handle.net/10415/2429>
- [12] He, J., Liu, C., Xu, X., Li, Y., Wu, S., Xu, J. "Performance research on modified KCS (Kalina cycle system) 11 without throttle valve." *Energy*. 64, pp. 389-397. 2014. DOI: [10.1016/j.energy.2013.10.059](https://doi.org/10.1016/j.energy.2013.10.059)
- [13] Nag, P., Gupta, A. "Exergy analysis of the Kalina cycle." *Applied Thermal Engineering*. 18(6), pp. 427-439. 1998. DOI: [10.1016/S1359-4311\(97\)00047-1](https://doi.org/10.1016/S1359-4311(97)00047-1)
- [14] Sun, F., Zhou, W., Ikegami, Y., Nakagami, K., Su, X. "Energy-exergy analysis and optimization of the solar-boosted Kalina cycle system 11 (KCS-11)." *Renewable Energy*. 66, pp. 268-279. 2014. DOI: [10.1016/j.renene.2013.12.015](https://doi.org/10.1016/j.renene.2013.12.015)
- [15] Kanoğlu, M., Çengel, Y., Dinçer, İ. "Energy and Exergy Efficiencies." In: *Efficiency Evaluation of Energy Systems*. New York: Springer. 2012.
- [16] Bao J., Zhao, L. "Exergy analysis and parameter study on a novel auto-cascade Rankine cycle." *Energy*. 48(1), pp. 539-547. 2012. DOI: [10.1016/j.energy.2012.10.015](https://doi.org/10.1016/j.energy.2012.10.015)
- [17] Elsayed, A., Embaye, M., Raya, A.-D., Mahmoud, S., Rezk, A. "Thermodynamic performance of Kalina cycle system 11 (KCS11): feasibility of using alternative zeotropic mixtures." *International Journal of Low-Carbon Technologies*. 8(suppl 1), pp. i69-i78. 2013. DOI: [10.1093/ijlct/ctt020](https://doi.org/10.1093/ijlct/ctt020)
- [18] Zhao, P., Wang, J., Gao, L., Dai, Y. "Parametric analysis of a hybrid power system using organic Rankine cycle to recover waste heat from proton exchange membrane fuel cell." *International Journal of hydrogen energy*. 37(4), pp. 3382-3391. 2012. DOI: [10.1016/j.ijhydene.2011.11.081](https://doi.org/10.1016/j.ijhydene.2011.11.081)
- [19] Khazaei, I., Ghazikhani, M., Mohammadiun, M. "Experimental and thermodynamic investigation of a triangular channel geometry PEM fuel cell at different operating conditions." *Scientia Iranica*. 19(3), pp. 585-593. 2012. DOI: [10.1016/j.scient.2011.11.039](https://doi.org/10.1016/j.scient.2011.11.039)
- [20] Chen, P.-C. "The dynamics analysis and controller design for the PEM fuel cell under gas flowrate constraints." *International Journal of Hydrogen Energy*. 36(4), pp. 3110-3122. 2011. DOI: [10.1016/j.ijhydene.2010.11.106](https://doi.org/10.1016/j.ijhydene.2010.11.106)
- [21] Leo, T., Durango, J., Navarro, E. "Exergy analysis of PEM fuel cells for marine applications." *Energy*. 35(2), pp. 1164-1171. 2010. DOI: [10.1016/j.energy.2009.06.010](https://doi.org/10.1016/j.energy.2009.06.010)
- [22] Al-Sulaiman, F. A., Dincer, I., Hamdullahpur, F. "Exergy analysis of an integrated solid oxide fuel cell and organic Rankine cycle for cooling, heating and power production." *Journal of Power Sources*. 195(8), pp. 2346-2354. 2010. DOI: [10.1016/j.jpowsur.2009.10.075](https://doi.org/10.1016/j.jpowsur.2009.10.075)
- [23] Yilanci, A., Dincer, I., Ozturk, H. "Performance analysis of a PEM fuel cell unit in a solar-hydrogen system." *International Journal of Hydrogen Energy*. 33(24), pp. 7538-7552. 2008. DOI: [10.1016/j.ijhydene.2008.10.016](https://doi.org/10.1016/j.ijhydene.2008.10.016)
- [24] Hettiarachchi, H. M., Golubovic, M., Worek, W. M., Ikegami, Y. "The performance of the Kalina cycle system 11 (KCS-11) with low-temperature heat sources." *Journal of Energy Resources Technology*. 129(3), pp. 243-247. 2007. DOI: [10.1115/1.2748815](https://doi.org/10.1115/1.2748815)